Effect of V_2O_5 Modification in V_2O_5/TiO_2-ZrO_2 Catalysts on Their Surface Properties and Catalytic Activities for Acid Catalysis

Jong Rack Sohn* **and Cheul Kyu Lee**

Department of Applied Chemistry, Engineering College, Kyungpook National University, Daegu 702-701, Korea
**E-mail: jrsohn@knu.ac.kr*
Received August 2, 2007

V_2O_5/TiO_2-ZrO_2 catalyst modified with V_2O_5 was prepared by adding $Ti(OH)_4$-$Zr(OH)_4$ powder into an aqueous solution of ammonium metavanadate followed by drying and calcining at high temperatures. The characterization of prepared catalysts was performed using XRD, DSC, solid-state ^{51}V NMR, and FTIR. In the case of calcination temperature of 500 °C, for the catalysts containing low loading V_2O_5 below 25 wt % vanadium oxide was in a highly dispersed state, while for catalysts containing high loading V_2O_5 equal to or above 25 wt % vanadium oxide was well crystallized due to the V_2O_5 loading exceeding the formation of monolayer on the surface of TiO_2-ZrO_2. The strong acid sites were formed through the bonding between dispersed V_2O_5 and TiO_2-ZrO_2. The larger the dispersed V_2O_5 amount, the higher both the acidity and catalytic activities for acid catalysis.

Key Words : V_2O_5 modification effect, Dispersed V_2O_5 amount, 2-Propanol dehydration, Cumene dealkylation

Introduction

Vanadium oxide catalysts are widely used as catalysts in oxidation reactions, *e.g.*, the oxidation of sulfur dioxide, carbon monoxide, and hydrocarbons.[1-5] These systems have also been found to be effective catalysts for the oxidation of methanol to methylformate.[6,7] Vanadia catalysts supported on titania-alumina mixed oxide and titania modified with alumina were found to exhibit superior activities in selective catalytic reduction of NOx.[8-11] Much research has been done to understand the nature of active sites, the surface structure of catalysts as well as the role played by the promoter of the supported catalysts, using infrared (IR), X-ray diffraction (XRD), electron spin resonance (E.S.R) and Raman spectroscopy.[7,12-14]

It is well known that the dispersion and the structural features of supported species can strongly depend on the support. Structure and other physicochemical properties of supported metal oxides are considered to be in different states compared with bulk metal oxides because of their interaction with the supports. Therefore, to achieve good activity and selectivity levels, V_2O_5 should be dispersed on a suitable support.[15] Titania in the form of anatase[16,17] is considered to be the more successful support for the phthalic anhydride production from *o*-xylene. Similarly, highest activity in methanol oxidation has been observed using ZrO_2 as the support.[18] Thus, the supporting metal oxide plays in determining the dispersion and activity of the V_2O_5 when supported.

On the other hand, binary metal oxides are expected to exhibit better catalytic activity for some reaction due to their solid acid or base properties.[19] Among various binary oxide, the TiO_2-ZrO_2 exhibited very good catalytic activity. The TiO_2-ZrO_2 binary oxide has also been reported to exhibit high surface acidity by a charge imbalance based on the generation of Ti-O-Zr bonding.[20] Further, recent studies also reveal that TiO_2-ZrO_2 is an active catalyst for dehydrocyclization of *n*-paraffins to aromatics,[21] hydrogenation of carboxylic acids to alcohols[22] and photo catalytic oxidation of acetone,[23] and also is an effective support for MoO_3-based catalysts for hydroprocessing application.[24] Thus, the combined TiO_2-ZrO_2 oxide has attracted attention recently as a catalyst and support for various applications.

Previously,[25] we reported solid-state ^{51}V NMR and IR spectroscopic study of V_2O_5 supported on TiO_2-ZrO_2. In this investigation, we report the effect of V_2O_5 modification in V_2O_5/TiO_2-ZrO_2 catalysts on their surface properties and catalytic activities for acid catalysis. 2-propanol dehydration and cumene dealkylation reactions were used as test reactions for acid catalysis.

Experimental Section

Catalyst Preparation. The coprecipitate of $Ti(OH)_4$-$Zr(OH)_4$ was obtained by adding aqueous ammonia slowly into a mixed aqueous solution of titanium tetrachloride and zirconium oxychloride at room temperature with stirring until the pH of mother liquor reached about 8. The ratio of titanium tetrachloride to zirconium oxychloride was 1:1, because TiO_2-ZrO_2 containing TiO_2/ZrO_2 ratio of 1 among TiO_2-ZrO_2 binary oxides exhibited the highest acidity and surface area.[26] The coprecipitate thus obtained was washed thoroughly with distilled water until chloride ion was not detected, and was dried at 100 °C for 12 h. The dried coprecipitate was powdered below 100 mesh.

The catalysts containing various vanadium oxide content were prepared by adding the $Ti(OH)_4$-$Zr(OH)_4$ powder into an aqueous solution of ammonium metavanadate (NH_4VO_3)

followed by drying and calcining at high temperatures for 3 h in air. This series of catalysts are denoted by their weight percentage of V_2O_5. For example, 10-V_2O_5/TiO_2-ZrO_2 indicates the catalyst containing 10 wt % V_2O_5.

Procedure. 2-Propanol dehydration was carried out at 160 and 180 °C in a pulse microreactor connected to a gas chromatograph. Fresh catalyst in the reactor made of 1/4 in. stainless steel was pretreated at 400 °C for 1 h in the nitrogen atmosphere. Pulses of 1 μL 2-propanol were injected into a N_2 gas stream which passed over 0.05 g of catalyst. Packing material for the gas chromatograph was diethyleneglycol succinate on Shimalite and column temperature was 150 °C. Catalytic activity for 2-propanol dehydration was represented as the mol of propylene converted per gram of catalyst.

Cumene dealkylation was carried out at 400 and 450 °C in the same reactor as above. Packing material for the gas chromatograph was Benton 34 on chromosorb W and column temperature was 130 °C. Catalytic activity for cumene dealkylation was represented as the mol of benzene converted from cumene per gram of catalyst. Conversion for both reactions was taken as the average of the first to sixth pulse values.

Chemisorption of ammonia was employed as a measure of acid amount of catalysts. The amount of chemisorption was obtained as the irreversible adsorption of ammonia.[27-29] The specific surface area was determined by applying the BET method to the adsorption of nitrogen at −196 °C.

FTIR absorption spectra of V_2O_5/TiO_2-ZrO_2 powders were measured by the KBr disk method over the range 1200-400 cm^{-1}. The samples for the KBr disk method were prepared by grinding a mixture of the catalyst and KBr powders in an agate mortar and pressing them in the usual way. FTIR spectra of ammonia adsorbed on the catalyst were obtained in a heatable gas cell at room temperature using a Mattson Model GL 6030E spectrophotometer. The self-supporting catalyst wafers contained about 9 mg/cm^2. Prior to obtaining the spectra the samples were heated under vacuum at 400-500 °C for 2 h.

Catalysts were checked in order to determine the structure of the support as well as that of vanadium oxide by means of a Jeol Model JDX-8030 diffractometer, employing Cu Kα (Ni-filtered) radiation.

DSC measurements were performed by a PL-STA model 1500H apparatus in air, and the heating rate was 5 °C per min. For each experiment, 10-15 mg of sample was used.

^{51}V NMR spectra were measured by a Varian Unity Inova 300 spectrometer with a static magnetic field strength of 7.05 T. Larmor frequency was 78.89 MHz. The ordinary single pulse sequence was used, in which the pulse width was set at 2.8 s and the acquisition time was 0.026 s. The spectral width was 500 kHz. The number of scans was varied from 200 to 15,000, depending on the concentration of vanadium. The signal was acquired from the time point 4 μs after the end of the pulse. The sample was static, and its temperature was ambient (21 °C). The spectra were expressed with the signal of $VOCl_3$ being 0 ppm, and the higher frequency shift from the standard was positive. Practically, solid NH_4VO_3 (−571.5 ppm) was used as the second external reference.[30,31]

Results and Discussion

Infrared Spectra of V_2O_5/TiO_2-ZrO_2. IR spectra of V_2O_5/TiO_2-ZrO_2 catalysts with various V_2O_5 contents calcined at 500 °C for 3 h were examined (This figure is not shown here). Although with catalysts below 25 wt % of V_2O_5 the definite peaks were not observed, the absorption bands at 1022 and 820 cm^{-1} appeared for 25-V_2O_5/TiO_2-ZrO_2, 33-V_2O_5/TiO_2-ZrO_2, and pure V_2O_5 containing high V_2O_5 content. The band at 1022 cm^{-1} is assigned to the V=O stretching vibration, while that at 820 cm^{-1} is attributable to the coupled vibration between V=O and to V-O-V.[32] Generally, the IR band of V=O in crystalline V_2O_5 shows at 1020-1025 cm^{-1} and the Raman band at 995 cm^{-1}.[2,33] The intensity of the V=O absorption gradually decreased with decreasing V_2O_5 content, although the band position did not change. The catalysts at vanadia loadings below 25 wt % gave no absorption bands due to crystalline V_2O_5. This observation suggests that vanadium oxide below 25 wt % is in a highly dispersed state. It is reported that V_2O_5 loading exceeding the formation of monolayer on the surface of support is well crystallized and observed in the spectra of IR and ^{51}V solid state NMR.[31]

^{51}V Solid State NMR Spectra of V_2O_5/TiO_2-ZrO_2. Solid state NMR methods represent a novel and promising approach to vanadium oxide catalytic materials. The solid state ^{51}V NMR spectra of V_2O_5/TiO_2-ZrO_2 catalysts calcined at 500 °C are shown in Figure 1 (This figure is also shown in other paper[25]). There are three types of signals in the spectra of catalysts with varying intensities depending on V_2O_5 content. At the low loadings up to 15 wt% V_2O_5 a shoulder at about −260 ppm and the intense peak at −590 ~ −730 ppm are observed. The former is assigned to the surface vanadium-oxygen structures surrounded by a distorted octahedron of oxygen atoms, while the latter is attributed to the tetrahedral vanadium-oxygen structures.[34-36]

However, the surface vanadium oxide structure is remarkably dependent on the metal oxide support material. Vanadium oxide on TiO_2 (anatase) displays the highest tendency to be 6-coordinated at low surface coverages, while in the case of γ-Al_2O_3 a tetrahedral surface vanadium species is the favored.[35] As shown in Figure 1, at low vanadium loading on TiO_2-ZrO_2 a tetrahedral vanadium species is exclusively dominant compared with a octahedral species. In general, it is known that low surface coverages favor a tetrahedral coordination of vanadium oxide, while at higher surface coverages vanadium oxide becomes increasingly octahedral-coordinated. As shown in Figure 1, the peak shapes for the vanadium species on TiO_2-ZrO_2 are narrower and more symmetric compared to those of vanadium species on TiO_2 or γ-Al_2O_3 reported by other reporters.[35,36] It seems likely that the different physical and chemical properties of TiO_2-ZrO_2 from those of TiO_2 or γ-Al_2O_3 affect the symmetry of the surface vanadium-oxygen structures.

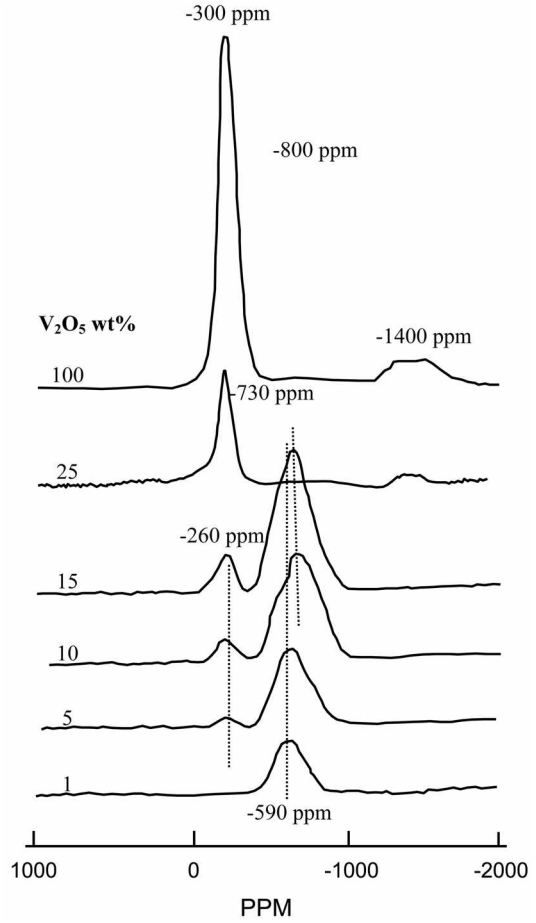

Figure 1. Solid state ^{51}V NMR spectra of V_2O_5/TiO_2-ZrO_2 catalysts calcined at 500 °C.

Increasing the V_2O_5 content on the TiO_2-ZrO_2 surface changes the shape of the spectrum to a rather intense and sharp peak at about −300 ppm ($\delta_\perp$) and a broad low-intensity peak at about −1400 ppm ($\delta_\parallel$), which are due to the crystalline V_2O_5 of square pyramid coordination.[35] These observations of crystalline V_2O_5 for samples containing high V_2O_5 content above 15 wt % are in good agreement with the results of the IR spectra. Namely, this is because V_2O_5 loading exceeding the formation of monolayer on the surface of TiO_2-ZrO_2 is well crystallized.[31]

Moreover, the increase in V_2O_5 content resulted appearance of additional signals with a peak at −730 ppm. The intensity of the signal increases with increase in V_2O_5 loading. Different peak positions normally indicate the differences of the spectral parameters and are observed due to different local environments of vanadium nuclei.[35-39] Thus species at −590 ppm and −730 ppm can be attributed to two types of tetrahedral vanadium complexes with different oxygen environments. Namely, the signals at −590 ppm can be attributed to the surface vanadium complexes containing OH groups or water molecules in their coordination sphere,[36] because the evacuation treatment decreases the intensities remarkably. On the other hand, the signals at −730 ppm are due to the surface tetrahedral vanadium complexes which do not contain OH groups or adsorbed water molecules.

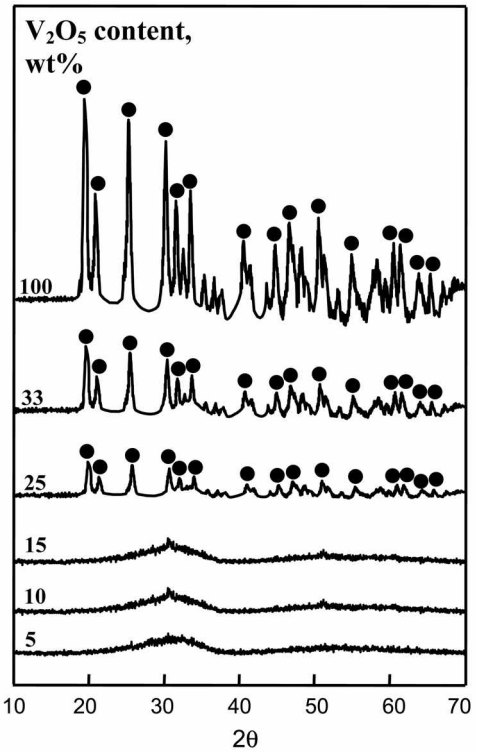

Figure 2. X-ray diffraction patterns of V_2O_5/TiO_2-ZrO_2 containing different V_2O_5 contents and calcined at 500 °C for 3 h: (●), orthorhomic phase of V_2O_5.

Crystalline Structure of V_2O_5/TiO_2-ZrO_2. The XRD patterns of the TiO_2-ZrO_2 support calcined at 500-1000 °C was examined. The TiO_2-ZrO_2 mixed support is in an amorphous state up to its 600 °C calcination temperature. However, the formation of the crystalline $ZrTiO_4$ compound was observed from 700 °C, and the line intensity of this compound increased with the calcination temperature. Recently, Fung and Wang[21] also reported the formation of the $ZrTiO_4$ compound at 650 °C and above temperature, coinciding with our XRD observations. The $ZrTiO_4$ compound appeared to be thermally quite stable even up to 1000 °C of calcination temperature.

The crystalline structure of V_2O_5/TiO_2-ZrO_2 containing different V_2O_5 contents and calcined in air at 500 °C for 3 h was checked by X-ray diffraction; the result are illustrated in Figure 2. TiO_2-ZrO_2 was amorphous to X-ray diffraction, indicating that the crystallization of $ZrTiO_4$ componud did not occur at 500 °C. These results are in good agreement with those of other invesitigors,[21] who reported the formation of crystalline $ZrTiO_4$ compound at 650 °C and above. V_2O_5 was amorphous to X-ray diffraction up to 15 wt% of V_2O_5, indicating good dispersion on the surface of catalyst. However, for V_2O_5/TiO_2-ZrO_2 containing high V_2O_5 content equal to or above 25 wt%, an orthorhombic phase of V_2O_5 was observed, showing that the amount of crystalline V_2O_5 increased with increasing V_2O_5 content, as shown in Figure 2. This is because V_2O_5 loading exceeding the formation of monolayer on the surface of support is well crystallized.

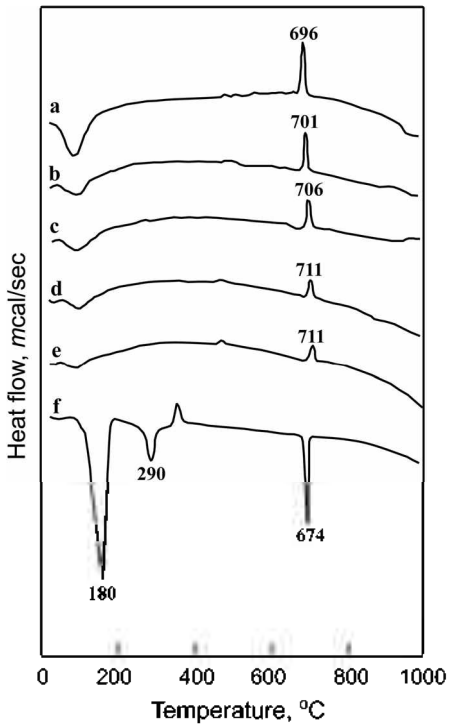

Figure 3. DSC curves of V_2O_5/TiO_2-ZrO_2 precursors containing different V_2O_5 contents: (a) TiO_2-ZrO_2, (b) 5-V_2O_5/TiO_2-ZrO_2, (c) 10-V_2O_5/TiO_2-ZrO_2, (d) 15-V_2O_5/TiO_2-ZrO_2, (e) 25-V_2O_5/TiO_2-ZrO_2, and (f) NH_4VO_3.

These results are in good agreement with those of infrared spectra and ^{51}V solid state NMR (Figure 1).

Thermal Analysis. To examine the thermal properties of precursors of V_2O_5/TiO_2-ZrO_2 samples more clearly, thermal analysis has been carried out; the results are illustrated in Figure 3. For NH_4VO_3 the DSC curve shows two endothermic peaks at 181 and 290 °C due to the evolution of NH_3 and H_2O decomposed from NH_4VO_3, indicating that the decompositon of NH_4VO_3 occurs in two steps. The sharp and endothermic peak at 674 °C is described to the melting of V_2O_5.[31]

However, for TiO_2-ZrO_2 and V_2O_5/TiO_2-ZrO_2 samples, the DSC patterns are somewhat different from that of NH_4VO_3. For TiO_2-ZrO_2, the DSC curve shows a broad endothermic peak below 200 °C due to the elimination of adsorbed water, and a sharp and exothermic peak at 696 °C due to the formation of $ZrTiO_4$ compound described in X-ray diffraction patterns. However, it is of interest to see the influence of V_2O_5 on the crystallization of $ZrTiO_4$ from amorphous to orthorhombic phase. As Figure 3 shows, the exothermic peak due to the crystallization appears at 696 °C for TiO_2-ZrO_2, while for V_2O_5/TiO_2-ZrO_2 samples it is shifted to higher temperatures. The shift increases with increasing V_2O_5 content up to 15 wt %. Consequently, the exothermic peaks appear at 701 °C for 5-V_2O_5/TiO_2-ZrO_2, 706 °C for 10-V_2O_5/TiO_2-ZrO_2, 711 °C for 15-V_2O_5/TiO_2-ZrO_2, and 711 °C for 25-V_2O_5/TiO_2-ZrO_2. It was shown that the addition of V_2O_5 as a second oxide to TiO_2-ZrO_2 hinders the crystallization of the originally amorphous preparation.[40]

Table 1. Specific surface area and acidity of V_2O_5/TiO_2-ZrO_2 containing different V_2O_5 contents and calcined at 500 °C for 3 h

Catalyst	Surface area, m^2/g	Acidity, μmol/g
TiO_2	52	80
ZrO_2	64	71
TiO_2-ZrO_2	201	168
3-V_2O_5/TiO_2-ZrO_2	226	199
5-V_2O_5/TiO_2-ZrO_2	231	212
10-V_2O_5/TiO_2-ZrO_2	250	234
15-V_2O_5/TiO_2-ZrO_2	247	256
25-V_2O_5/TiO_2-ZrO_2	221	227
33-V_2O_5/TiO_2-ZrO_2	186	197

For the catalysts above 15 wt % of V_2O_5, however, the shift of transition temperature did not occur more successively. For the samples above 15 wt %, no further shift of transition temperature means that the content of V_2O_5 exceeding 15 wt % does not interact with the surface of TiO_2-ZrO_2.

Surface Properties of Catalysts. The specific surface areas and acidity of catalysts calcined at 500 °C for 3 h are listed in Table 1. Thermal resistance of zirconia against sintering can be considerably improved by incorporation of a second oxide.[41,42] As listed in Table 1, the surface area and acidity of TiO_2-ZrO_2 binary oxide increased remarkably compared with pure titania and zirconia. It has been reported that high surface acidity of TiO_2-ZrO_2 binary oxide is attributed to the charge imbalance based on the generation of Ti-O-Zr bonding.[20] Yu *et al.* has shown that TiO_2-ZrO_2 binary metal oxide exhibits higher catalytic activity than pure TiO_2, possibly due to an increase in surface area at a given calcination temperature and an increase in acidity.[42] The presence of V_2O_5 also influences the surface area and acidity. The surface area and acidity increase gradually with

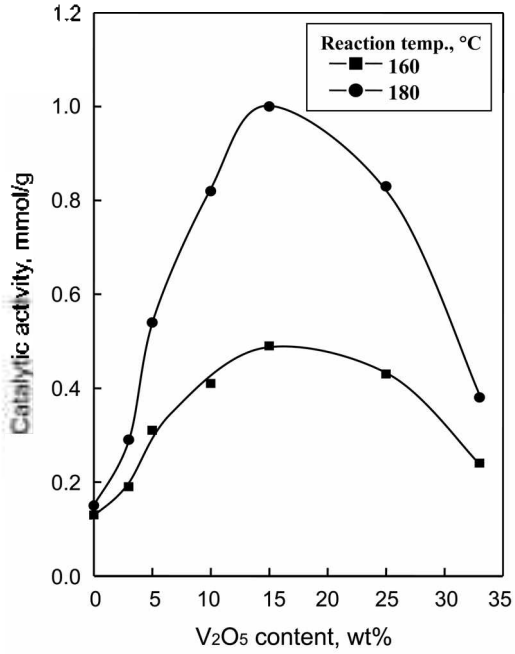

Figure 4. Catalyric activity of V_2O_5/TiO_2-ZrO_2 for 2-propanol dehydration as a function of V_2O_5 content.

increasing V_2O_5 loading up to 15 wt%. It seems likely that the interaction between V_2O_5 and TiO_2-ZrO_2 prevents catalysts from crystallizing.[31] The decrease of surface area for V_2O_5/TiO_2-ZrO_2 containing V_2O_5 above 15 wt % is also due to the blocking of TiO_2-ZrO_2 pores by the increased V_2O_5 loading. It seems likely that strong acid sites are formed through the bonding between dispersed V_2O_5 and TiO_2-ZrO_2. Similary to the case of catalysts modified with WO_3 and MoO_3,[44,45] the new acid sites can be formed and the acid strength can be strongly enhanced by the inductive effect of vanadium oxide species bonded to the surface of catalyst. The surface area attained a maximum for 10-V_2O_5/TiO_2-ZrO_2, while the acidity attained a maximum for 15-V_2O_5/TiO_2-ZrO_2.

We obtained the infrared spectra of ammonia adsorbed on 15-V_2O_5/TiO_2-ZrO_2 catalyst evacuated at 500 °C for 1 h to examine the nature of acidic sites. The band at 1454 cm^{-1} is the characteristic peak of an ammonium ion, which is formed on the Brönsted acid sites; the absorption peak at 1620 cm^{-1} is contributed by ammonia coordinately bonded to Lewis acid sites,[46,47] indicating the presence of both Brönsted and Lewis acid sites on the surface of the 15-V_2O_5/TiO_2-ZrO_2 catalyst. Other samples having different V_2O_5 content also showed the presence of both Lewis and Brönsted acids. Therefore, these V_2O_5/TiO_2-ZrO_2 catalysts can be used as catalysts for Lewis or Brönsted acid catalysis.

Catalytic Activities for Acid Catalysis. The catalytic activity of V_2O_5/TiO_2-ZrO_2 calcined at 500 °C for the 2-propanol dehydration is measured; the results are illustrated as a function of the V_2O_5 content in Figure 4, where reaction temperature is 160-180 °C. In view of Table 1 and Figure 4, the variation in the catalytic activity for 2-propanol dehydration can be correlated with the change of its acidity, showing the highest activity and acidity for 15-V_2O_5/TiO_2-ZrO_2. It has been known that 2-propanol dehydration takes place very readily on weak acid sites.[24,48-50] Good correlations have been found in many cases between the acidity and the catalytic activities of solid acids. For example, the rates of both the catalytic decomposition of cumene and the polymerization of propylene over SiO_2-Al_2O_3 catalysts were found to increase with increasing acid amount at acid strength $H_0 \leq +3.3$.[51] It was also reported that the catalytic activity of nickel silicates in the ethylene dimerization as well as in the butene isomerization was closely correlated with the acid amount of the catalyst.[52]

Catalytic activity for cumene dealkylation against the V_2O_5 content are presented in Figure 5, where reaction temperature is 400-450 °C. The catalytic activity increased with increasing the V_2O_5 content, reaching a maximum at 15 wt% similar to the results of 2-propanol dehydration in Figure 4. Comparing Table 1 and Figure 5, the catalytic activity is also correlated with the acidity of catalyst. The correlation between catalytic activity and acidity holds for both reactions, cumene dealkylation and 2-propanol dehydration, although the acid strength required to catalyze acid reaction is different depending on the type of reactions.[28,48-50] As seen in Figures 4 and 5, the catalytic activity for cumene dealkylation, in spite of higher reaction temperature, is not higher than that for 2-propanol dehydration. It is also remarkable that the catalysts without V_2O_5 exhibit low catalytic activities for both 2-propanol dehydration and cumene dealkylation, indicating that V_2O_5 component plays an important role in the formation of acid sites and the increased catalytic activities for both reactions. The catalytic activities of V_2O_5/TiO_2-ZrO_2 for both reactions are similar to those of ZrO_2/MoO_3 modified with MoO_3 reported previously.[53] Poisoning by coke is a common problem in catalysis over acid-catalysts. For V_2O_5/TiO_2-ZrO_2, the catalytic activities for both reactions decreased very slowly due to the coke formation.

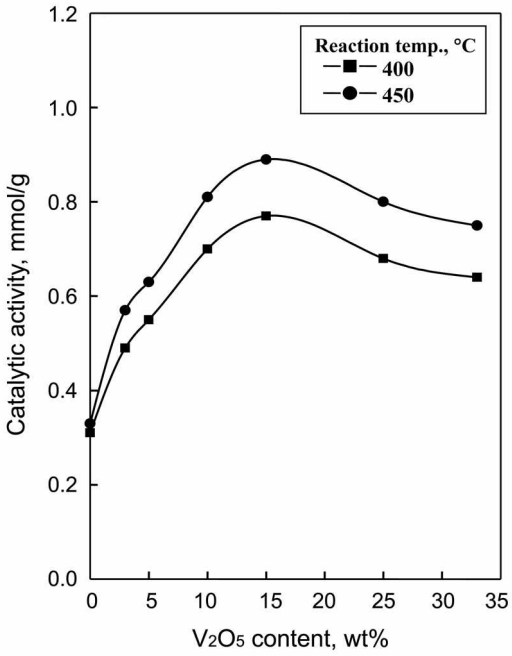

Figure 5. Catalytic activity of V_2O_5/TiO_2-ZrO_2 for cumene dealkylation as a function of V_2O_5 content.

Effect of Dispersed V_2O_5 Amount on Acidity and Catalytic Activity. The forms of active components present in heterogeneous catalysts are of importance to catalysis. A great many oxides can disperse spontaneously onto the surface of supports to form a monolayer, because the monolayer is a thermodynamically stable form.[54] We can measure the amount of dispersed V_2O_5 from the results of IR, ^{51}V NMR, and XRD. Dispersed V_2O_5 amount, surface area, acidity are listed in Table 2. There are good correlations among the dispersed V_2O_5 amount, acidity, and catalytic activity. Namely, the larger the dispersed V_2O_5 amount, the higher both acidity and catalytic activity. This can be explained in terms of that strong acid sites are formed through the bonding between dispersed V_2O_5 and TiO_2-ZrO_2 and consequently catalytic activity increases due to the increased acid sites.

The catalytic activities for 2-propanol dehydration at 180 °C and cumene dealkylation at 450 °C are also listed in Table 2. The maximum activities for both reactions are obtained

Table 2. Dispersed V_2O_5 amount, specific surface area, acidity, and catalytic activity for acid catalysis of V_2O_5/TiO_2-ZrO_2

Catalyst	Dispersed V_2O_5 amount, V_2O_5(g)/TiO_2-ZrO_2(g)	Surface area, m^2/g	Acidity, μmol/g	Catalytic activity, mmol/g	
				2-Propanol dehydration	Cumene dealkylation
TiO_2-ZrO_2	0	201	168	0.15	0.33
3-V_2O_5/TiO_2-ZrO_2	0.03	226	199	0.29	0.57
5-V_2O_5/TiO_2-ZrO_2	0.05	231	212	0.54	0.63
10-V_2O_5/TiO_2-ZrO_2	0.10	250	234	0.82	0.81
15-V_2O_5/TiO_2-ZrO_2	0.16	247	256	1.00	0.89

Table 3. Dispersed V_2O_5 amount, acidity, and turnover frequency for acid catalysis of V_2O_5/TiO_2-ZrO_2

Catalyst	Dispersed V_2O_5 amount, V_2O_5(g)/TiO_2-ZrO_2(g)	Acidity, μmol/g	Turnover frequency, mmol/mmol	
			2-Propanol dehydration	Cumene dealkylation
TiO_2-ZrO_2	0	168	0.89	1.96
3-V_2O_5/TiO_2-ZrO_2	0.03	199	1.46	2.86
5-V_2O_5/TiO_2-ZrO_2	0.05	212	2.55	2.97
10-V_2O_5/TiO_2-ZrO_2	0.10	234	3.50	3.46
15-V_2O_5/TiO_2-ZrO_2	0.16	256	3.90	3.48

with the 15-V_2O_5/TiO_2-ZrO_2 catalyst containing 15 wt% V_2O_5, where the amount of dispersed V_2O_5 is also maximum. It seems likely that the highest activity of the catalyst containing 15 wt% V_2O_5 is related to its acidity and acid strength. The high acid strength and acidity are responsible for the V=O bond nature of complex formed by the interaction between V_2O_5 and TiO_2-ZrO_2.[55] This isolated V_2O_5 species is stabilized through multiple V-O-Zr(Ti) bonds between each vanadium oxide species and the TiO_2-ZrO_2 surface.[56,57] As listed in Tables 1 and 2, the acidity of 15-V_2O_5-/TiO_2-ZrO_2 is the most among the catalysts. Of course, the acidity of catalysts is related to their specific surface area, as mentioned above. In fact, Tables 1 and 2 show that the specific surface area attained a maximum when the V_2O_5 content in V_2O_5/TiO_2-ZrO_2 is 10-15 wt%. Although the activity of sample without V_2O_5 was low as acid catalyst, as shown in Figures 4 and 5, the V_2O_5/TiO_2-ZrO_2 with V_2O_5 exhibited high catalytic activity for acid catalysis.

We checked the turnover frequency of V_2O_5/TiO_2-ZrO_2 catalysts for both reactions, that is, the catalytic activity per acid site and the results are listed in Table 3. As listed in Table 3, the turnover frequency for both reactions also increased with increasing the dispersed V_2O_5 amount, implying that the acid strength of V_2O_5/TiO_2-ZrO_2 increased with the dispersed V_2O_5 amount. The turnover frequency of TiO_2-ZrO_2 without V_2O_5 is very low compared with that of V_2O_5/TiO_2-ZrO_2 modified with V_2O_5. Therefore, it is clear that V_2O_5 modification increases the acid strength of modified V_2O_5/TiO_2-ZrO_2.

Conclusions

This paper has shown that a combination of FTIR, XRD, DSC and ^{51}V solid-state NMR can be used to perform the characterization of V_2O_5/TiO_2-ZrO_2 catalysts modified with V_2O_5. On the basis of results of FTIR, XRD, and solid state ^{51}V NMR, at low calcination temperature of 500 °C vanadium oxide up to 15 wt% was well dispersed on the surface of TiO_2-ZrO_2. However, high V_2O_5 loading (equal to or above 25 wt%) exceeding the formation of monolayer on the surface of TiO_2-ZrO_2 was well crystallized. The strong acid sites were formed through the bonding between dispersed V_2O_5 and TiO_2-ZrO_2. The larger the dispersed V_2O_5 amount, the higher both the acidity and catalytic activities for acid catalysis.

Acknowledgement. We wish to thank Kora Basic Science Institute(Daegu Branch) for the use of X-ray diffractometer.

References

1. Nakagawa, Y.; Ono, T.; Miyata, H.; Kubokawa, Y. *J. Chem. Soc., Faraday Trans. 1* **1983**, *79*, 2929.
2. Miyata, H.; Kohno, M.; Ono, T.; Ohno, T.; Hatayama, F. *J. Chem. Soc. Faraday Trans. 1* **1989**, *85*, 3663.
3. Reddy, B. M.; Ganesh, I.; Chowdhury, B. *Catal. Today* **1999**, *49*, 115.
4. Lakshmi, L. J.; Ju, Z.; Alyea, E. C. *Langmuir* **1999**, *15*, 3521.
5. Doh, I. J.; Pae, Y. I.; Sohn, J. R. *J. Ind. Eng. Chem.* **1999**, *5*, 161.
6. Forzatti, P.; Tronoconi, E.; Busca, G.; Titarellp, P. *Catal. Today* **1987**, *1*, 209.
7. Busca, G.; Elmi, A. S.; Forzatti, P. *J. Phys. Chem.* **1987**, *91*, 5263.
8. Centi, G.; Militerno, S.; Perathoner, S.; Riva, A.; Barambilla, G. *J. Chem. Soc. Chem. Commun.* **1991**, 88.
9. Centi, G.; Perathoner, S.; Kartheuser, B.; Rohan, D.; Hoidnett, B. K. *Appl. Catal. B* **1992**, *1*, 129.
10. Matralis, H. M.; Ciardelli, M.; Ruwet, M.; Grange, P. *J. Catal.* **1995**, *157*, 368.
11. Mastikhin, V. M.; Terskikh, V. V.; Lapina, O. B.; Filiminova, S. V.; Seidl, M.; Knovinger, H. *J. Catal.* **1995**, *156*, 1.
12. Elmi, A. S.; Tronoconi, E.; Cristiani, C.; Martin, J. P. G.; Forzatti, P. *Ind. Eng. Chem. Res.* **1989**, *84*, 237.
13. Miyata, H.; Fujii, K.; Ono, T.; Kubokawa, Y.; Ohno, T.; Hatayama, F. *J. Chem. Soc., Faraday Trans. 1* **1987**, *83*, 675.
14. Cavani, F.; Centi, G.; Foresti, E.; Trifiro, F. *J. Chem. Soc., Faraday Trans. 1* **1988**, *84*, 237.
15. Bond, G. C.; Tahir, S. F. *Appl. Catal.* **1991**, *71*, 1.
16. Wachs, I. E.; Saleh, R. Y.; Chan, S. S.; Chersich, C. *Chemtech* **1985**, 756.

17. Wong, W. C.; Nobe, K. *Ind. Eng. Chem. Prod. Res. Dev.* **1984**, *23*, 563.
18. Roozeboom, F.; Cordingley, P. D.; Gellings, P. J. *J. Catal.* **1981**, *68*, 464.
19. Tanabe, K.; Sumiyoshi, T.; Shibata, K.; Kiyoura, T.; Kitagawa, J. *Bull. Chem. Soc. Jpn.* **1974**, *47*, 1064.
20. Wu, J. C.; Chung, C. S.; Ay, C. L.; Wang, I. *J. Catal.* **1984**, *87*, 98.
21. Fung, J.; Wang, F. *J. Catal.* **1991**, *130*, 577.
22. Reddy, E. P.; Rojas, T. C.; Fernández, A. *Langmuir* **2000**, *16*, 4217.
23. Zorn, M. E.; Tompkins, D. T.; Zeltner, W. A.; Anderson, M. A. *Appl. Catal. B: Environmental* **1999**, *23*, 1.
24. Miciukiewicz, J.; Mang, T.; Knözinger, H. *Appl. Catal. A* **1995**, *122*, 151.
25. Park, E. H.; Lee, M. H.; Sohn, J. R. *Bull. Korean Chem. Soc.* **2000**, *21*, 913.
26. Sohn, J. R.; Lee, S. H. *Catal. Lett.* **2007**, *118*, 203.
27. Sohn, J. R.; Lee, S. G.; Shin, D. C. *Bull. Korean Chem. Soc.* **2006**, *27*, 1623.
28. Sohn, J. R.; Kim, H. W.; Lim, J. S. *J. Ind. Eng. Chem.* **2006**, *12*, 104.
29. Sohn, J. R.; Lee, S. H. *Appl. Catal. A:Gen.* **2004**, *266*, 89.
30. Hayashi, S.; Hayamizu, K. *Bull. Chem. Soc. Jpn.* **1990**, *63*, 961.
31. Sohn, J. R.; Cho, S. G.; Pae, Y. I.; Hayashi, S. *J. Catal.* **1996**, *159*, 170.
32. Mori, K.; Miyamoto, A.; Murakami, Y. *J. Chem. Soc. Faraday Trans.* **1987**, *83*, 3303.
33. Bjorklund, R. B.; Odenbrand, C. U. I.; Brandin, J. G. M.; Anderson, L. A. H.; Liedberg, B. *J. Catal.* **1989**, *119*, 187.
34. Roozeboom, F.; Mittelmelijer-Hazeleger, M. C.; Moulijn, J. A.; Medema, J.; de Beer, U. H. J.; Gelling, P. J. *J. Phys. Chem.* **1980**, *84*, 2783.
35. Eckert, H.; Wachs, I. E. *J. Phys. Chem.* **1989**, *93*, 6796.
36. Reddy, B. M.; Reddy, E. P.; Srinivas, S. T.; Mastikhim, V. M.; Nosov, N. V.; Lapina, O. B. *J. Phys. Chem.* **1992**, *96*, 7076.
37. Le Costumer, L. R.; Taouk, B.; Le Meur, M.; Payen, E.; Guelton, M.; Grimblot, J. *J. Phys. Chem.* **1988**, *92*, 1230.
38. Narsimha, K.; Reddy, B. M.; Rao, P. K.; Mastikhin, V. M. *J. Phys. Chem.* **1990**, *94*, 7336.
39. Sobalik, Z.; Lapina, O. B.; Novgorodova, O. N.; Mastikhin, V. M. *Appl. Catal.* **1990**, *63*, 191.
40. Pae, Y. I.; Lee, S. H.; Sohn, J. R. *Catal. Lett.* **2005**, *99*, 241.
41. Mercera, P. D. L.; van Ommen, J. G.; Doesburg, E. B. M.; Burggraaf, A. J.; Ross, J. R. H. *Appl. Catal.* **1990**, *57*, 127.
42. Sohn, J. R.; Ryu, S. G. *Langmuir* **1993**, *9*, 126.
43. Yu, J. C.; Lin, J.; Kwok, R. W. M. *J. Phys. Chem. B* **1998**, *102*, 5094.
44. Sohn, J. R.; Park, M. Y. *Langmuir* **1998**, *14*, 6140.
45. Sohn, J. R.; Kwon, S. H.; Shin, D. C. *Appl. Catal. A:Gen.* **2007**, *317*, 216.
46. Sohn, J. R.; Han, J. S.; Kim, H. W.; Pae, Y. I. *Bull. Korean Chem. Soc.* **2005**, *26*, 755.
47. Satsuma, A.; Hattori, A.; Mizutani, K.; Furuta, A.; Miyamoto, A.; Hattori, T.; Murakami, Y. *J. Phys. Chem.* **1988**, *92*, 6052.
48. Sohn, J. R.; Jang, H. J. *J. Mol. Catal.* **1991**, *64*, 349.
49. Decanio, S. J.; Sohn, J. R.; Paul, P. O.; Lunsford, J. H. *J. Catal.* **1986**, *10*, 132.
50. Sohn, J. R.; Han, J. S.; Lim, J. S. *J. Ind. Eng. Chem.* **2004**, *1*, 1003.
51. Tanabe, K. *Solid Acids and Bases*; Kodansha: Tokyo, 1970; p 103.
52. Sohn, J. R.; Ozaki, A. *J. Catal.* **1980**, *6*, 29.
53. Sohn, J. R.; Chun, E. W.; Pae, Y. I. *Bull. Korean Chem. Soc.* **2003**, *24*, 1785.
54. Xie, Y. C.; Tang, Y. Q. *Adv. Catal.* **1990**, *37*, 1.
55. Arata, K. *Adv. Catal.* **1990**, *37*, 165.
56. Liu, Z.; Chen, Y. *J. Catal.* **1998**, *177*, 314.
57. Chen, K.; Xie, S.; Iglesia, E.; Bell, A. T. *J. Catal.* **2000**, *189*, 421.